Multicenter character in single-electron emission from H_2 molecules by ion impact

M. E. Galassi* and R. D. Rivarola
Instituto de Física Rosario (CONICET-UNR), Av. Pellegrini 250, 2000 Rosario, Argentina

P. D. Fainstein
Centro Atómico Bariloche, Comisión Nacional de Energia Atómica, Avda E. Bustillo 9500, 8400 Bariloche, Argentina
(Received 19 March 2004; published 29 September 2004)

Single ionization cross sections for heavy-ion impact on H_2 are calculated by applying the continuum-distorted-wave–eikonal-initial-state model. We have used a representation of the bound-state initial wave function which takes into account the molecular character of the target. To describe the final continuum state we have used the two-effective-center approximation, previously employed with success to study electron capture from H_2 by ion impact. Interference effects are also analyzed and the dependence of the oscillation frequency with the projectile velocity and ejection angle is presented. The importance of adequately describing the target as a molecule is emphasized.

DOI: 10.1103/PhysRevA.70.032721 PACS number(s): 34.50.Fa, 34.50.Gb

I. INTRODUCTION

Knowledge of differential and total ionization cross sections of atoms and molecules by protons and heavier ions is of great interest in many areas such as atmospheric, plasma, and biological physics. In particular, hydrogen plays a major role in some of the hottest environments either found in nature or artificially made, such as stars or fusion reactors. An important heating mechanism of these systems is due to the thermalization of ^{4}He particles continuously produced by $^2H+^3H$ or $^2H+^2H$ fusion reactions. The understanding of the way in which the atomic and nuclear interactions involving these particles takes place is a key factor to model such systems. To achieve this goal, cross sections corresponding to the different possible reactions must be obtained in the laboratory. However, in these experiments, atomic hydrogen is rarely found without being mixed with molecular hydrogen. Then, the knowledge of collision processes involving H_2 molecules is a necessary step to model the progress of particles in hydrogenic gases media.

The process of ion impact electron emission from atomic targets has been studied in great detail since the 1960s. Nowadays perturbative models based on distorted-wave theory are able to describe the process with very good accuracy [1–3]. On the contrary, in the case of molecular targets current theoretical methods are far from reaching the same level of success as for atomic targets. This is mostly due to the geometrical structure of the molecule which breaks the simpler symmetry of atoms and to the difficulty of including a good description of the electronic structure of the molecule together with the dynamics of the collisions.

In a previous work we have calculated the single ionization cross sections of several molecular targets (N_2, O_2, CO, CH_4) by proton impact [4] employing two different approximations: Bragg's additivity rule, where the molecule is considered as a sum of atoms, and a molecular representation of the initial target bound state. In the latter, the cross section was approximated by a linear combination of atomic cross sections with coefficients determined from a population analysis and binding energies extracted from experimental spectra. Deviation were found with respect to the additivity rule showing therefore the importance of taking into account the molecular character of the target. However, the geometry of the molecule was not taken into account and, in the final continuum state, we considered that the electron evolved in a static Coulomb potential generated by the effective interaction of the ejected electron with the nuclei and electrons of the residual target as a whole (one-center approximation).

Recent experimental findings [5] have shown evidence of interference patterns in the electron emission spectra produced in collisions between fast highly charged ions with H_2. These results have been explained as interference from the coherent emission from the proximities of the two nuclei of the molecule [5–7] which can only be represented theoretically by including in the model the two-center character of the molecular target.

In the present work we will develop a theoretical model of single ionization of H_2 by ion impact. The improvement with respect to our previous work is the inclusion, within the two-effective center approximation, of the two-center character of the molecule. For this purpose we follow previous work for single electron capture from molecular hydrogen [8]. A short account of the model with an application to study interference effects has been given a short while ago [6]. Here we present the full development of the theory, its applications to the calculation of differential and total cross sections, and to more recent results which provide evidence of interference effects. Atomic units will be used except when otherwise stated.

II. THEORY

The basic difficulty in modeling the single ionization process in ion-atom or ion-molecule collisions at intermediate to high energies arises from the long range of the Coulomb

*Electronic address: galassi@fceia.unr.edu.ar

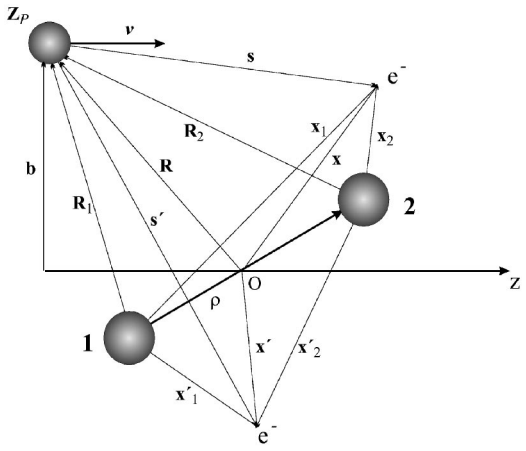

FIG. 1. Reference system.

interaction between all charged particles. In the initial channel, the projectile field will distort the initial bound state, while in the final channel, the emitted electron will travel in the combined fields of the residual target and projectile. Furthermore, there is an additional difficulty introduced by the fact that the target is a multielectronic atom or molecule. A convenient way to treat this problem in perturbation theory is through the distorted-wave formalism and by reducing the many-body problem to that of one active electron in some model potential [9].

Let us consider the single ionization of molecular hydrogen by impact of a bare nucleus of charge Z_P and velocity $\mathbf{v}$. In what follows, we will work within the straight-line version of the impact parameter method. We will consider that the internuclear vector of H_2 remains fixed during the reaction, and the rotation and vibration of the nuclei will be ignored (this assumption is valid for collision times smaller than the vibrational time). Therefore the molecular orientation appears as an additional degree of freedom, and the average over all possible molecular alignments must be considered to obtain differential and total cross sections.

The total Hamiltonian of the system is given by

$$H = -\frac{1}{2}\nabla_{\mathbf{x}}^2 - \frac{1}{2}\nabla_{\mathbf{x}'}^2 - \frac{Z_T}{x_1} - \frac{Z_T}{x_2} - \frac{Z_T}{x_1'} - \frac{Z_T}{x_2'} - \frac{Z_P}{s} - \frac{Z_P}{s'} + \frac{1}{|\mathbf{x}-\mathbf{x}'|} + \frac{Z_P Z_T}{R_1} + \frac{Z_P Z_T}{R_2}, \tag{1}$$

where Z_T is the nuclear charge of each one of the nuclei of the target (in this work Z_T=1). The middle point O of the internuclear vector ρ is taken as the origin of the laboratory reference system (see Fig. 1). The coordinates $\mathbf{x}$, $\mathbf{x}_1$, $\mathbf{x}_2$, and $\mathbf{s}$ correspond to the electron to be ionized (active electron), whereas the primed coordinates correspond to the nonionized electron (passive electron). $\mathbf{R}_1$ and $\mathbf{R}_2$ are the coordinates of the impinging ion with respect to each nuclei of the molecular target. Working in the distorted-wave formalism, the post version of the first-order transition amplitude can be written as

$$\mathcal{A}_{if}^{+}(\boldsymbol{\rho},\mathbf{b}) = -i\int_{-\infty}^{+\infty} dt \left\langle \Psi_f^{-} \left| \left(H - i\frac{\partial}{\partial t}\right)^{\dagger} \right| \Psi_i^{+} \right\rangle, \tag{2}$$

where Ψ_i^+ and Ψ_f^- are the initial and final distorted-wave functions in the entrance and exit channels, respectively, and $\mathbf{b}$ is the impact parameter referred to the point O.

Within the independent electron approximation, the distorted-wave functions are written as a product of wave functions corresponding to the active and passive electrons. We also assume that the passive electron remains *frozen* in its initial orbital $\varphi_i^p(\mathbf{x}')$ during the collision. The initial and final total wave functions are then proposed as

$$\Psi_{i,f}^{+,-}(\mathbf{x},\mathbf{x}',t) = \zeta_{i,f}^{+,-}(\mathbf{x},t)\varphi_i^p(\mathbf{x}'). \tag{3}$$

We now define a new Hamiltonian $\tilde{H}$ averaged over the passive electron wave function φ_i^p:

$$\tilde{H} = \langle \varphi_i^p | H | \varphi_i^p \rangle = \tilde{H}_a + V_s(\mathbf{R},\boldsymbol{\rho}) + \varepsilon_p, \tag{4}$$

where

$$\tilde{H}_a = -\frac{1}{2}\nabla_{\mathbf{x}}^2 - \frac{Z_T}{x_1} - \frac{Z_T}{x_2} - \frac{Z_P}{s} + V_{ap}(\mathbf{x},\boldsymbol{\rho}) \tag{5}$$

represents the active electron Hamiltonian,

$$V_s(\mathbf{R},\boldsymbol{\rho}) = \left\langle \varphi_i^p \left| -\frac{Z_P}{s'} + \frac{Z_P Z_T}{R_1} + \frac{Z_P Z_T}{R_2} \right| \varphi_i^p \right\rangle \tag{6}$$

is the static potential between the projectile and the residual H_2^+ ion,

$$V_{ap}(\mathbf{x},\boldsymbol{\rho}) = \left\langle \varphi_i^p \left| \frac{1}{|\mathbf{x}-\mathbf{x}'|} \right| \varphi_i^p \right\rangle \tag{7}$$

represents the interaction between the electrons and

$$\varepsilon_p = \left\langle \varphi_i^p \left| -\frac{1}{2}\nabla_{\mathbf{x}'}^2 - \frac{Z_T}{x_1'} - \frac{Z_T}{x_2'} \right| \varphi_i^p \right\rangle \tag{8}$$

is the passive electron energy.

From Eq. (4) it results that $\tilde{H}$ is a monoelectronic Hamiltonian describing the dynamics of the active electron. The static potential V_s depends only on $\mathbf{R}$ and $\boldsymbol{\rho}$. Therefore, as it is well known, it can be taken into account through phase factors [1]. If we define the wave functions

$$\zeta_i^+(\mathbf{x},t) = \chi_i^+(\mathbf{x},t)\exp(-i\varepsilon_p t)\exp\left(-i\int_{-\infty}^{t} dt' V_s(\mathbf{R},\boldsymbol{\rho})\right), \tag{9}$$

$$\zeta_f^-(\mathbf{x},t) = \chi_f^-(\mathbf{x},t)\exp(-i\varepsilon_p t)\exp\left(i\int_{t}^{+\infty} dt' V_s(\mathbf{R},\boldsymbol{\rho})\right), \tag{10}$$

the transition amplitude $\mathcal{A}_{if}^+$ can be written as

$$\mathcal{A}_{if}^{+}(\rho,\mathbf{b}) = \exp\left(-i\int_{-\infty}^{+\infty} dt'\ V_s(\mathbf{R},\boldsymbol{\rho})\right) A_{if}^{+}(\boldsymbol{\rho},\mathbf{b}), \tag{11}$$

where

$$\mathcal{A}_{if}^{+}(\boldsymbol{\rho},\mathbf{b}) = -i\int_{-\infty}^{+\infty} dt \left\langle \chi_f^{-} \left| \left(\tilde{H}_a - i\frac{\partial}{\partial t}\right)^{\dagger} \right| \chi_i^{+} \right\rangle. \quad (12)$$

In the present work we are only interested in the calculation of differential cross sections, as a function of electron emission angle and energy, and of total cross section. These are obtained from the integration of the square modulus of the transition amplitude. Thus the phase factor appearing in Eq. (11) gives no contribution. Therefore the internuclear interaction has no effect, within the impact parameter approximation, on the cross sections which depend on the electron angle and energy. We can therefore work with the transition amplitude A_{if}^{+} given by Eq. (12).

The initial and final distorted-wave functions for the active electron are proposed as

$$\chi_{i,f}^{+,-} = \Phi_{i,f}\mathcal{L}_{i,f}^{+,-}, \quad (13)$$

where Φ_i and Φ_f are the initial and final time-dependent bound and continuum wave functions and $\mathcal{L}_i^{+}$ and $\mathcal{L}_f^{-}$ the corresponding distortions. These multiplicative distortion factors take into account the interaction between the projectile and the active electron and thus can be chosen as in the atomic target case. In the present case we will use the continuum-distorted-wave–eikonal–initial-state (CDW-EIS) model which has been applied with great success to atomic targets [9,10]. In this model, which we label CDW-EIS-MO to indicate that it accounts for the molecular geometry, the distortion factors are given by

$$\mathcal{L}_i^{+EIS} = \exp\left(-i\frac{Z_P}{v}\ln(vs + \mathbf{v}\cdot\mathbf{s})\right), \quad (14)$$

$$\mathcal{L}_f^{-CDW} = N^{\star}\left(\frac{Z_P}{p}\right)_1 F_1\left(-i\frac{Z_P}{p};1;-ips - i\mathbf{p}\cdot\mathbf{s}\right) \quad (15)$$

for the initial and final states, respectively. In Eq. (15), $\mathbf{p}$ is the electron momentum in the projectile frame and $N(a) = \exp(\pi a/2)\Gamma(1+ia)$.

The time-dependent bound and continuum-wave functions of the active electron are solutions of the following Schrödinger equation:

$$\left[-\frac{1}{2}\nabla_{\mathbf{x}}^2 - \frac{Z_T}{x_1} - \frac{Z_T}{x_2} + V_{ap}(\mathbf{x},\mathbf{b}) - i\frac{\partial}{\partial t}\right]\Phi_{i,f}(\mathbf{x},t) = 0. \quad (16)$$

In the present formulation we approximate $\Phi_i(\mathbf{x},t)$ by a single-ζ wave function [8] which can be written as a sum of orbitals $\phi_{1,2}$ centered on each nuclei of the molecule (the same representation is used for the initial bound state of the passive electron):

$$\Phi_i(\mathbf{x},t) \cong [\phi_1(\mathbf{x}_1) + \phi_2(\mathbf{x}_2)]e^{-i\varepsilon_i t}, \quad (17)$$

where the molecular orbital energy is given by $\varepsilon_i = E_i - \varepsilon_P$, with E_i the total electronic molecular energy. The orbitals are given by

$$\phi_j(\mathbf{x}_j) = N_i(\rho)\left(\frac{Z^3}{\pi}\right)^{1/2} e^{-Zx_j}; \quad j = 1,2 \quad (18)$$

with $N_i(\rho) = 0.5459$ a normalization factor corresponding to the equilibrium internuclear distance $\rho = 1.4$ a.u. and $Z = 1.193$. Replacing Eqs. (13) and (17) in Eq. (12), we obtain

$$\mathcal{A}_{if}^{+}(\boldsymbol{\rho},\mathbf{b}) = -i\int_{-\infty}^{+\infty} dt \langle \Phi_f \mathcal{L}_f^{-CDW} | W_f^{\dagger} | \phi_1 L_i^{+EIS} \rangle e^{-i\varepsilon_i t} - i\int_{-\infty}^{+\infty} dt \langle \Phi_f \mathcal{L}_f^{-CDW} | W_f^{\dagger} | \phi_2 \mathcal{L}_i^{+EIS} \rangle e^{-i\varepsilon_i t}, \quad (19)$$

where W_f is the perturbative potential. As can be seen from Eq. (19), the molecular transition amplitude $A_{if}^{+}(\boldsymbol{\rho},\mathbf{b})$ is equal to a sum of two transition amplitudes which can be associated to the ionization process from effective bound states centered on nucleus 1 and 2, respectively. We now use the two-effective center model, previously employed with success to study electron capture from H_2 by ion impact [8,11] and electron emission from H_2 by electron impact [12], and assume that when the active electron is emitted from a region close to the nucleus 1 (2), the passive electron charge screens completely the charge of nucleus 2 (1). The continuum wave function $\Phi_f(\mathbf{x},t)$ in the first (second) term is replaced by a function $\Phi_f^1(\mathbf{x}_1,t)[\Phi_f^2(\mathbf{x}_2,t)]$ that describes the active electron in the field of center 1 (2). In this way, we neglect the influence of nucleus 2 (1) and the passive electron in the choice of the continuum function in the exit channel within the first (second) term. These approximations allows to avoid the problem of working with two-center integrals. The molecular continuum is then given by

$$\Phi_f^j(\mathbf{x}_j,t) = \phi_f(\mathbf{x}_j)\exp(-i\epsilon_f t + i\beta_j\mathbf{k}\cdot\boldsymbol{\rho}/2); \quad j = 1,2, \quad (20)$$

where $\mathbf{k} \equiv (k,\theta_e,\varphi_e)(\epsilon_f = k^2/2)$ is the ejected electron momentum (energy), $\beta_1 = -1$, $\beta_2 = +1$, and

$$\phi_f(\mathbf{x}_j) = (2\pi)^{-3/2} e^{i\mathbf{k}\cdot\mathbf{x}_j} N^{\star}(\gamma^{\star})_1 F_1(-i\gamma^{\star};1;-ikx_j - i\mathbf{k}\cdot\mathbf{x}_j), \quad (21)$$

where $\gamma^{\star} = Z_{eff}/k$ and $Z_{eff} = \sqrt{-2\varepsilon_i}$. Using this approximation we finally obtain that

$$A_{if}^{+}(\boldsymbol{\rho},\mathbf{b}) \cong \sum_{j=1}^{2} e^{-i\beta_j(\mathbf{k}\cdot\boldsymbol{\rho} - q_z\rho_z)/2} A_{if}^{eff,+}(\boldsymbol{\rho},\mathbf{b}_j), \quad (22)$$

with $\mathbf{b}_j$ the impact parameter with respect to the molecular center j and $q_z = \Delta\varepsilon_{fi}/v$ (with $\Delta\varepsilon_{fi} = \varepsilon_f - \varepsilon_i$) the z component, taken in the projectile's direction, of the momentum transfer $\mathbf{q} = -\boldsymbol{\eta} - q_z\hat{v}$. The vector $\boldsymbol{\eta} \equiv (\eta,\varphi_\eta)$ is the transverse component of the momentum transfer. The functions $A_{if}^{eff,+}$ are transition amplitudes corresponding to effective atoms located at the position of each molecular center:

$$A_{if}^{eff,+}(\boldsymbol{\rho},\mathbf{b}_j) = -i\int_{-\infty}^{+\infty} dt\langle\Phi_f^j\mathcal{L}_f^{-CDW}|W_{f,j}^{\dagger}|\phi_j e^{-i\epsilon_i t}\mathcal{L}_i^{+EIS}\rangle, \tag{23}$$

where $W_{f,1}$ and $W_{f,2}$ are the perturbative potentials corresponding to each molecular center given by

$$W_{f,j}^{CDW}\chi_{f,j} = \Phi_f^j(\mathbf{x}_j,t)\{\nabla_{x_j}\ln[{}_1F_1(-i\xi^*;1;-ikx_j - i\mathbf{k}\cdot\mathbf{x}_j)]\cdot\nabla_s\mathcal{L}_f^{-CDW}\} \tag{24}$$

The main result from the model now appears in Eq. (22). The transition amplitude is given by a coherent sum of effective scattering processes taking place on each molecular center. The relative phase is given by the exponential term which will contain therefore all the information about interference effects.

Instead of the scattering amplitude (23) it is more convenient to work with its Fourier transform whose square modulus is given by

$$|R_{if}^{+}(\boldsymbol{\eta},\boldsymbol{\rho})|^2 = 2\{1+\cos[(\mathbf{k}+\mathbf{q})\cdot\boldsymbol{\rho}]\}|R_{if}^{eff,+}(\boldsymbol{\eta})|^2, \tag{25}$$

where $R_{if}^{eff,+}$ is the Fourier transform of $A_{if}^{eff,+}$. Averaging over all molecular orientations we obtain the final expression for the doubly differential cross section as a function of electron energy and solid angle ($d\Omega$):

$$\frac{d^2\sigma}{d\epsilon_f d\Omega} = 8\pi k\int d\eta\left(1+\frac{\sin(|\mathbf{k}+\mathbf{q}|\rho)}{|\mathbf{k}+\mathbf{q}|\rho}\right)|R_{if}^{eff,+}(\eta)|^2 = S_d(\varepsilon_f,\Omega)+S_i(\varepsilon_f,\Omega) \tag{26}$$

which involves the integration over the transverse momentum transfer. As we have made explicit in Eq. (26), the doubly differential cross section can be written as a sum of direct (S_d) and interference (S_i) terms.

III. RESULTS AND DISCUSSIONS

A. Doubly differential cross sections

In order to test the model, we have made some calculations for proton and highly charged ion impact on H_2 at intermediate and high energies.

In Fig. 2 we present the doubly differential cross sections (DDCS's) for fixed emission angles as a function of the ejected electron energy for 114-keV H^+ impact on H_2 calculated with the CDW-EIS-MO approximation in comparison with experimental data [13]. Also presented in the figure are calculations performed with the first Born (B1) and CDW-EIS models using Bragg's additivity rule. As expected, both CDW-EIS calculations are in better agreement with experiments. From the comparison of the calculations with atomic or molecular wave functions it appears that for this system the differences in absolute magnitude are small. It is important to note that CDW-EIS-MO gives the best agreement at low electron energies where the cross section has the largest values.

For backward emission both atomic and molecular CDW-EIS calculations underestimate the DDCS experimental data at high enough electron energies. This behavior, which has been previously observed for He targets using the CDW-EIS approximation [24], has been attributed to the sensitive of DDCS, at large emission angles, with the description of the bound and continuum target wave functions [24,25]. In order to improve the agreement between theory and experiment, numerical exact molecular bound and continuum-wave functions could be used. However, it implies an extremely difficult computational task, which is out of the scope of the present paper.

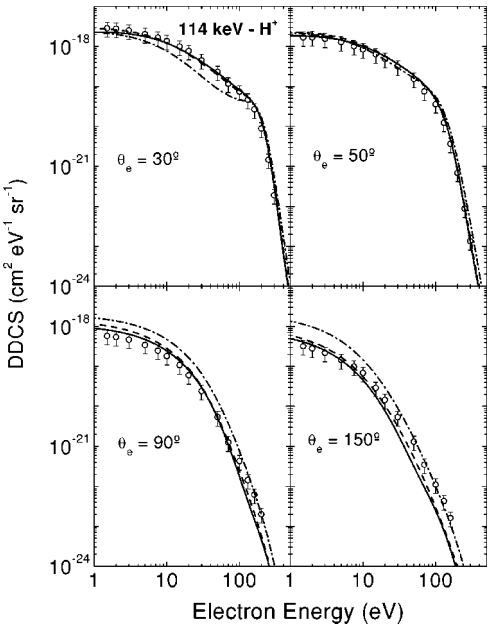

FIG. 2. DDCS for single ionization of H_2 by 114-keV proton impact as a function of the electron energy for fixed values of the electron angle. Theory: solid line, CDW-EIS-MO; dashed line, CDW-EIS; dash-dotted line, B1. Experiments: (○), from Ref. [13].

In Figs. 3 and 4 the DDCS as a function of electron energy for 60-MeV/u Kr^{34+} and 68-MeV/u Kr^{33+} impact on H_2 are compared with experimental data [5,14]. For the calculation the projectile charge is taken equal to the ionic charge. This is a good approximation because the projectile electrons belong to the inner shells and are tightly bound. Both atomic

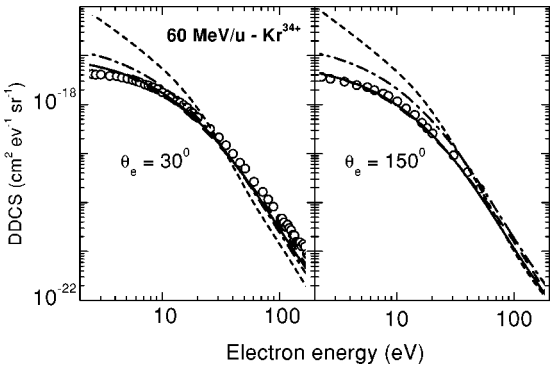

FIG. 3. DDCS for single ionization of H_2 by 60-MeV/u Kr^{34+} impact as a function of the electron energy for fixed values of the electron angle. Theory: solid line, CDW-EIS-MO; dashed line, CDW-EIS; dash-dotted line, B1; short-dash, results from Ref. [7]. Experiments: (○), from Ref. [5].

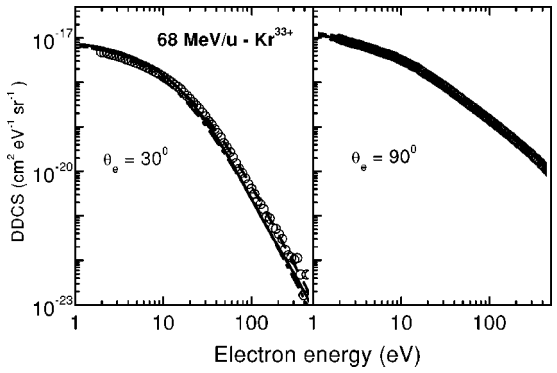

FIG. 4. DDCS for single ionization of H_2 by 68-MeV/u Kr^{33+} impact as a function of the electron energy for fixed values of the electron angle. Theory: solid line, CDW-EIS-MO; dashed line, CDW-EIS; dash-dotted line, B1. Experiments: (○), from Ref. [14].

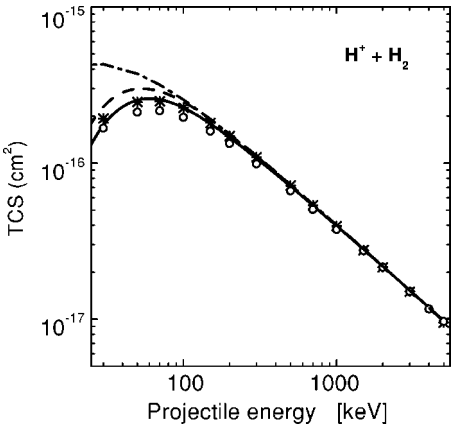

FIG. 5. TCS for single ionization of H_2 by proton impact as a function of the projectile energy. Theory: solid line, CDW-EIS-MO; dashed line, CDW-EIS; dash-dotted line, B1. ○, recommended data from Ref. [17]; stars, experimental data from Ref. [16].

and molecular CDW-EIS calculations are in good agreement with the experimental data. It is interesting to note that even though the impact energy is very large, due to the high value of the projectile charge, the use of perturbative models where the projectile potential is not included in the initial and final wave functions can be a matter of discussion. Therefore it is not surprising that the first Born approximation gives the worst results for the 60-MeV/u Kr^{34+} case. As in the calculation for proton impact the differences between CDW-EIS and CDW-EIS-MO are quite small.

In Fig. 3 we have also included the theoretical results from Ref. [7]. This calculation uses the semiclassical model based on the first Born approximation [15] assuming that the initial state is a linear combination of 1s-type atomic orbitals centered at each of the nuclei and the final state is represented by plane waves. Significant discrepancies with the experiments are found at all electron energies. This is most probably related to the simple representation of the final continuum state and to the use of a peaking approximation, neglecting transverse momentum transfer contributions, which is not valid at small values of the electron energy.

B. Total cross sections

After integration of the doubly differential cross section over the electron energy and angle we obtain the total cross section (TCS). In Fig. 5 we present theoretical results from B1, CDW-EIS, and CDW-EIS-MO calculations in comparison with recommended values for single ionization of H_2 by proton impact [16,17]. Both calculations using the CDW-EIS model are in very good agreement with the recommended values at high impact energies. In the region of the maximum the best result is obtained with CDW-EIS-MO. This is due to the better description of the low electron-energy part of the spectra which gives the main contribution to the total cross section. It is well known that this part of the spectra is also sensitive to the potential used for the target, i.e., to the quality of the target wave functions used in the calculation. It appears therefore that the molecular wave function gives indeed a better representation of the bound state a trace of which can be seen even in the total cross sections. This is consistent with our previous findings [4] showing the limitations of Bragg's rule at intermediate impact energies. The B1 calculations overestimate the experimental data below 200-keV impact energy.

C. Interferences effects

As already mentioned before, it appears clearly in Eq. (26) that the cross section corresponding to molecular hydrogen present an oscillatory factor that arises from the coherent emission from the proximities of both nuclei of the molecule. These oscillations, also called interferences, can be related to those expected from a Young-type two-slit experiments [18,19]. However, it is not the diffracted projectile which follows different trajectories as it scatters on the two nuclei. This effect is not possible here due to the large mass of the projectile which makes its wave length very small. On the contrary, the continuous spectrum of emitted electron show the preference of ionization to be produced from the proximities of the molecular centers, according to the electron distribution of the H_2 ground state.

This type of interference effects, arising from the two-center character of the H_2 molecule, were first reported for single electron capture [20] and photoionization [21]. More recently, new results in photoionization [22,23], electronic capture [8,11,26,27] and electron emission by electrons impact [12,28] have allowed us to expand the knowledge about the process leading to experimental verification of the theory.

In the case of ion-impact single ionization, the first experimental evidence of interference effects was obtained for 60-MeV/u Kr^{34+} ions impinging on H_2 [5]. More recently evidence has been found at smaller impact energies [29]. Theoretical calculations made with different models [6,7] have been able to reproduce the general behavior of experimental findings and give support to the interpretation as an interference from coherent waves emitted from each molecular center.

The sum of amplitudes with different phases results within the present CDW-EIS-MO model in a DDCS which can be expressed as the sum of two different terms, S_d and S_i. They represent contributions from direct and interference

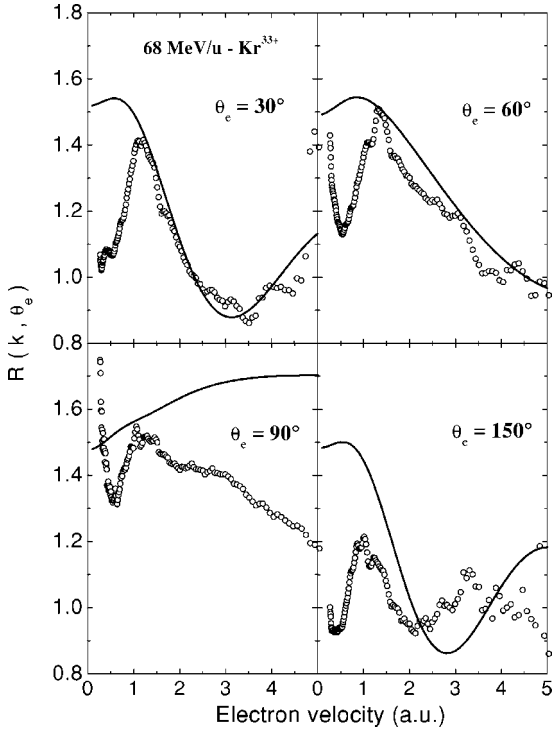

FIG. 6. Ratio of the DDCS for electron emission at 30°, 60°, 90°, and 150° from H_2 and 2-H atoms, for 68-MeV/amu Kr^{33+} impact as a function of the electron velocity. Experiment: (○), from Ref. [14]. Theory: solid line, present CDW-EIS-MO calculation.

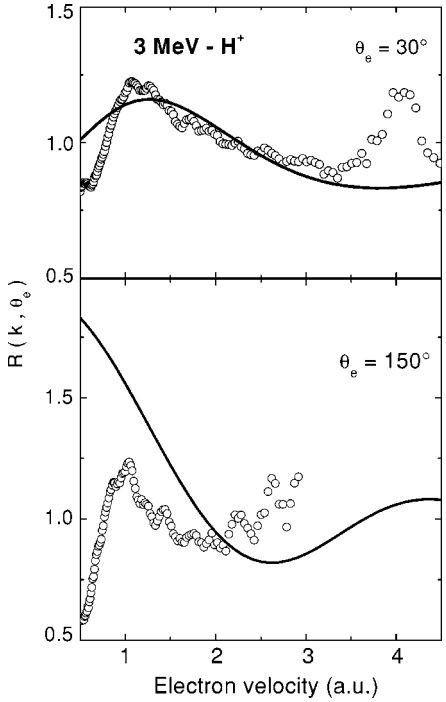

FIG. 7. Ratio of the DDCS for electron emission at 30° and 150° from H_2 and 2-H atoms, for 3-MeV proton impact as a function of the electron velocity. Experiment: (○), from Ref. [29]. Theory: solid line, present CDW-EIS-MO calculation.

processes, respectively. The main difference between S_d and S_i resides in the $\sin(|\mathbf{k}+\mathbf{q}|\rho)/(|\mathbf{k}+\mathbf{q}|\rho)$ term in the integrand of Eq. (26). This term depends on the molecular internuclear distance, the momentum transfer and the electron energy and angle. On the contrary S_d is independent of ρ. However, the DDCS is not appropriate to highlight the oscillations because it decreases monotonically by several orders of magnitude in the electron energy range of interest (see, for example, Fig. 2). Therefore it is better to plot the ratio $R(k,\theta_e)$ between the DDCS for ionization of H_2 and two times the DDCS for ionization of H. If there are no effects due to the structure of the molecule we can expect that, at the high impact energy considered here, the ratio will give a value close to 1 (it may differ from this value due to the different binding energies of H_2 and H, the effective charge Z_{eff} and the normalization of the bound-state wave functions).

In Fig. 6 we plot $R(k,\theta_e)$ as a function of electron velocity at fixed emission angles in comparison with the experimental data from [14] for 68-MeV/u Kr^{33+} impact on H_2. The same is plotted in Fig. 7 but in comparison with the data from [29] for 3-MeV H^+ impact. As in Refs. [5,29], for a better comparison, the calculations for H were made with the CDW-EIS model using different charges for the target nucleus in the entrance ($Z_T=1$) and exit ($Z_{eff}=1.19$ in Fig. 6 and $Z_{eff}=1.05$ in Fig. 7, respectively) channels and the experimental value of $\varepsilon_i=-0.566$ a.u. as it has being done to normalize experimental data. Theoretical CDW-EIS-MO calculations are not expected to give a good description of experimental cross section ratios at electron velocities lower than 1 a.u. In a recent work [23] it has been shown that in photoionization, to describe the abrupt fall of experimental data as the electron velocity decreases, it is necessary to use accurate bound and continuum electron target wave functions. In that work, these molecular wave functions were obtained numerically by using *B*-spline basis functions. Moreover, it was shown that structures below $k=1$ a.u. do not correspond to interference but to electron correlation and/or screening effects. Thus interference effects must be investigated for electron velocities larger than 1 a.u. In this velocity domain, the present CDW-EIS-MO model gives a good description of experimental data for 68-MeV/u Kr^{33+} impact at $\theta_e=30°$ and $\theta_e=60°$ and for 3-MeV H^+ impact at $\theta_e=30°$ where evidence of interference patterns is observed. The peak shown by experiments at $k=4$ a.u. for 3-MeV H^+ could be due to the large experimental uncertainty as k increases, according to the preliminary character of the measurements [29]. We have observed that for the $\theta_e=60°$ case, theoretical results (not shown in the figure) present, at larger emission velocities, an oscillatory behavior characteristic of the presence of interferences. For Kr^{33+} at $\theta_e=90°$ the agreement between theory and experiments is poorer. The origin of this discrepancy, also shown in calculations of Ref. [7], is not well understood. Experimental data and theoretical calculations shown in Fig. 6 for $\theta_e=90°$ present a weaker dependence with electron velocity compared with the ratios obtained for the other angular cases. This behavior has been attributed to the contribution of binary encounter electrons [14]. As in the $\theta_e=60°$, calculations for $\theta_e=90°$ show oscillations for larger electron velocities. For $\theta_e=150°$, in both Kr^{33+} and H^+ cases, experimental ratios present oscillation frequencies larger than the ones predicted by the theory. It could be due to the men-

TABLE I. Fit values of the frequency parameter c as a function of the electron emission angle θ_e.

θ_e	Experimental results from Ref. [14]	Theory from Ref. [7]: c_N	Present results: c_G
30°	0.96	0.87	0.98
60°	0.52	0.5	0.51
90°	0.29	0	
150°	1.46	0.87	1.105

tioned limitation of the validity of the CDW-EIS-MO model at backward emission angles.

To understand more quantitatively the interference structures, an analytical fit function of the form

$$R(k,\theta_e) = A\left(1 + \frac{\sin(ck\rho)}{ck\rho}\right) + B \tag{27}$$

was proposed [14]. In Eq. (27), A and B (with $A=B=0.5$) are interfering and noninterfering cross-section fractions, respectively, and c an adjustable frequency. The theoretical model from Ref. [7] predicts that $c=c_N=|k\cos(\theta_e)-q_z|/k$ which at the high impact energies considered here is given with good approximation by $c_N \approx \cos(\theta_e)$. In the CDW-EIS-MO approximation this frequency can also be found in closed analytical form. From Eq. (26) we see that the oscillatory term in the integrand presents a frequency $|\mathbf{k}+\mathbf{q}|/k$ where

$$|\mathbf{k}+\mathbf{q}|^2 = k^2 - k\left(\eta\sin(\theta_e)\cos(\varphi_\eta - \varphi_e) + \frac{\Delta\varepsilon}{v}\cos(\theta_e)\right) + q^2, \tag{28}$$

which depends on the transverse momentum transfer η, so that it is impossible to compare directly the results from CDW-EIS-MO and the experimental c value. We have to integrate over the transverse momentum transfer and then fit the ratios to extract a value of the frequency which can be compared with experiments. If we neglect the transverse momentum transfer in Eq. (28) we arrive at the approximate frequency $c_G \approx [k - q_z\cos(\theta_e)]/k$ which can be taken out from the integral. The first important result is that both theoretical models predict that the frequency depends on the emission angle. This effect was recently demonstrated in experiments [14]. However, we see that we can never retrieve the result of Ref. [7] as we cannot impose on our final result the approximations made in that calculation. The most striking result from the CDW-EIS-MO approximation is, however, that the frequency depends on the electron momenta k. This shows that it is in principle not possible to fit the whole function $R(k,\theta_e)$ with such a simple function. It can only be made in a restricted range of k values where for example the function makes just one oscillation. Using expression (27) we have therefore fitted our results obtained employing Eq. (26) in the k range covered by the experiments [14]. It permit us to determine precisely the frequency c_G given by CDW-EIS-MO. In Table I we show the results from this fitting in comparison with the experimental data for the 68-MeV/u $Kr^{33+}+H_2$ system and with the high-energy approximation to the theoretical results from Ref. [7].

We can see that the present theoretical results are in very good agreement with the experimental ones for $\theta_e=30°$ and 60° and show an improvement in comparison with the results from Ref. [7]. At 90° the dependence given by CDW-EIS-MO is very smooth and we were not able to fit these results with a simple function such as that given by Eq. (27). For backward angles theory and experiment are not in agreement. This is already expected from the results shown in Figs. 6 and 7. However, the value obtained from CDW-EIS-MO is larger than that given by c_N showing an asymmetry of the frequency between forward and backward angles. Therefore the whole functional dependence of the frequency on emission angle found in the experiment is qualitatively reproduced by CDW-EIS-MO.

The frequency of oscillation calculated with CDW-EIS-MO also depends on the projectile velocity (but not on the projectile charge). As we discussed at length in our previous work [6], as the projectile velocity decreases the ratios must be analyzed with care. It is well known that the DDCS presents characteristic structures: the electron capture to the continuum (CTC) and binary encounter (BE) peaks. The CTC peak rapidly disappears as the emission angle increases but the BEP remains at all forward angles. The position in the spectra of the BEP depends on the projectile velocity. In the experimental studies [5,14,29] performed so far the range of k values is limited to values smaller to those where the structures appears. If this range is fixed and the impact energy decreased it may happen that at a certain value the peak appears. The BEP depends on the Compton profile of the target, being therefore different for H and H_2. This difference can produce additional structures in the ratio which have no relation to the interference pattern. It is therefore not convenient to study this dependence with the function $R(k,\theta_e)$. We therefore define as in Ref. [6] a new ratio given by $R'(k,\theta_e)=(S_d+S_i)/S_d$ which avoids this problem because S_d and S_i present the same Compton profiles and just differ in the interference factor.

In Fig. 8 we show calculated values of $R'(k,\theta_e)$ as a function of the electron velocity for fixed emission angle, for different impact energies. In all cases we find a damped oscillatory behavior which asymptotically behaves as $R'(k,\theta_e)\to 1$ as $k\to\infty$. This behavior can be deduced from Eq. (26). The damping depends on the impact energy and it increases as the impact energy decreases. The frequency also depends on the impact energy and it is seen that it also increases with decreasing impact energy. Although we have taken care to eliminate all structures not related to the interference pattern, additional structures appear for 100-keV and 1-MeV impact energy at approximately 3 and 10.9 a.u., respectively (indicated by arrows in Fig. 8). It can be easily shown that these structures correspond to the binary encounter region. The binary peak appears when the whole momentum transfered from the projectile is taken by the electron (binary collision). This can be represented mathematically by the condition $\mathbf{k}=-\mathbf{q}$. In this case the interference factor takes its maximum value equal to 2 [see Eq. (26)].

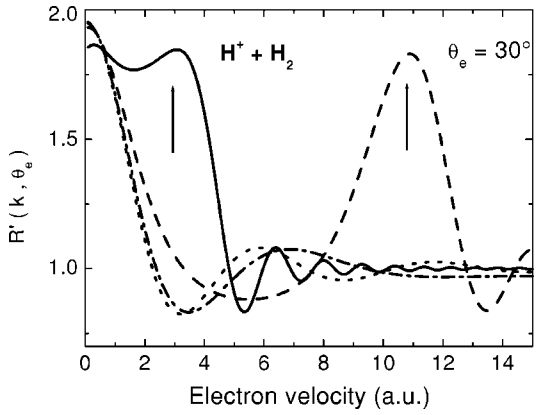

FIG. 8. Ratio $(S_d+S_i)/S_d$ for proton impact at a fixed angle of electron emission of 30°, for different projectile energies as a function of the electron velocity. Solid line, 100 keV; dashed line, 1 MeV; dash-dotted line, 10 MeV; dotted line, 60 MeV.

IV. CONCLUSIONS

We have presented a theoretical model to calculate doubly differential and total cross section for single electron emission from H_2 molecules by ion impact. The comparison with experimental and recommended DDCS's show that it is important to use a representation of the bound and continuum states, which take into account the two-center character of the molecule. Theoretical results give the general trend of experimental DDCS's.

A more detailed comparison is given when absolute DDCS's are divided by effective hydrogen DDCS's. It allows also the study of interference effects. The present theoretical model, as shown from recent calculations for photoionization, is not valid at electron velocities lower the 1 a.u., where screening and/or correlation effects dominate. Interference effects must be studied for larger electron velocities. A good description of experimental interferences is obtained for forward ionization. However, as the emission angle increases, the theoretical model fails to represent the existing experimental results, giving only their qualitative behavior.

We have also shown that the frequency of oscillations depends on the emitted electron energy, ejection angle, and projectile velocity. Therefore it is not possible to find a frequency depending only of the emitted electron angle to characterize the oscillations as it has been found in previous work.

To obtain a better representation of the studied ionization reaction, accurate molecular bound, and continuum wave functions must be employed, as it has been recently shown for photoionization [23]. For the larger electron velocity range considered here it implies an extremely difficult computational task, which is a matter of our future interest. At low electron velocities, the coupling of direct ionization with autoionizing two-electron channels as well as the coupling between direct ionization and the nuclear movement of the molecule should be considered in the theory. Work in this line is also in progress in our research group.

ACKNOWLEDGMENTS

We acknowledge Fundación Antorchas and Consejo Nacional de Investigaciones Científicas y Técnicas de Argentina for partial support.

[1] P. D. Fainstein, V. H. Ponce, and R. D. Rivarola, J. Phys. B **24**, 3091 (1991).
[2] N. Stolterfoht, R. D. DuBois, and R. D. Rivarola, *Electron Emission in Heavy Ion-Atom Collisions* (Springer-Verlag, Berlin, 1997).
[3] R. D. Rivarola and P. D. Fainstein, Nucl. Instrum. Methods Phys. Res. B **205**, 448 (2003).
[4] M. E. Galassi, R. D. Rivarola, M. Beuve, G. H. Olivera, and P. D. Fainstein, Phys. Rev. A **62**, 022701 (2000).
[5] N. Stolterfoht, B. Sulik, V. Hoffman, B. Skovall, J. Y. Chesnel, J. Rangama, F. Frémont, D. Hennecart, A. Cassimi, H. Husson, A. Landers, J. A. Tanis, M. E. Galassi, and R. D. Rivarola, Phys. Rev. Lett. **87**, 023201 (2001).
[6] M. E. Galassi, R. D. Rivarola, P. D. Fainstein, and N. Stolterfoht, Phys. Rev. A **66**, 052705 (2002).
[7] L. Nagy, L. Kocbach, K. Pora, and J. Hansen, J. Phys. B **35**, L453 (2002).
[8] H. F. Busnengo, S. E. Corchs, and R. D. Rivarola, Phys. Rev. A **57**, 2701 (1998).
[9] P. D. Fainstein, V. H. Ponce, and R. D. Rivarola, J. Phys. B **21**, 287 (1988).
[10] D. S. F. Crothers, and J. F. McCann, J. Phys. B **16**, 3229 (1983).
[11] S. E. Corchs, H. F. Busnengo, and R. D. Rivarola, Nucl. Instrum. Methods Phys. Res. B **149**, 247 (1999).
[12] P. Weck, O. A. Fojón, J. Hanssen, B. Joulakian, and R. D. Rivarola, Phys. Rev. A **63**, 042709 (2001).
[13] M. W. Gealy, G. W. Kerby III, Ying-Yuan Hsu, and M. E. Rudd, Phys. Rev. A **51**, 2247 (1995).
[14] N. Stolterfoht, B. Sulik, L. Gulyás, B. Skovall, J. Y. Chesnel, F. Frémont, D. Hennecart, A. Cassimi, L. Adoui, and J. A. Tanis, Phys. Rev. A **67**, 030702 (2003).
[15] J. P. Hansen and L. Kocbach, J. Phys. B **22**, L71 (1989).
[16] M. E. Rudd, R. D. DuBois, L. H. Toburen, C. A. Ratcliffe, and T. V. Goffe, Phys. Rev. A **28**, 3244 (1983).
[17] M. E. Rudd, Y.-K. Kim, D. H. Madison, and J. W. Gallagher, Rev. Mod. Phys. **57**, 965 (1985).
[18] T. Young, *A Course of Lectures on Natural Philosophy and the Mechanical Arts* (Joseph Johnson, London, 1807).
[19] R. Feynman, R. B. Leighton, and M. Sands, *The Feynman Lectures on Physics* (Addison-Wesley, Reading, MA, 1965), Vol. III.
[20] T. F. Tuan and E. Gerjuoy, Phys. Rev. **117**, 756 (1960).
[21] H. D. Cohen and U. Fano Phys. Rev. **50**, 30 (1966).
[22] M. Walter and J. Briggs, J. Phys. B **32**, 2487 (1999).
[23] O. A. Fojón, J. Fernández, A. Palacios, R. D. Rivarola, and F. Martín, J. Phys. B **37**, 3035 (2004).
[24] L. Gulyás, P. D. Fainstein, and A. Salin, J. Phys. B **28**, 245 (1995).
[25] D. H. Madison, Phys. Rev. A **8**, 2449 (1973).

[26] Y. D. Wang, J. H. McGuire, and R. D. Rivarola, Phys. Rev. A **40**, 3673 (1989).
[27] S. E. Corchs, R. D. Rivarola, J. H. McGuire, and Y. D. Wang, Phys. Scr. **50**, 469 (1994).
[28] C. R. Stia, O. A. Fojón, P. Weck, J. Hanssen and R. D. Rivarola, J. Phys. B **36**, L257 (2003).
[29] S. Hossain, A. S. Alnaser, A. L. Landers, D. J. Pole, H. Knutson, A. Robison, B. Stamper, N. Stolterfoht, and J. A. Tanis, Nucl. Instrum. Methods Phys. Res. B **205**, 484 (2003).